The actin cytoskeletal network plays a role in prion transmission and contributes to prion stability

Short title: Actin cytoskeletal networks contribute to prion stability

Jane E. Dorweiler*, Mitchell J. Oddo*, Douglas R. Lyke*, Jacob A. Reilly*, Brett T. Wisniewski*, Emily E. Davis*, Abigail M. Kuborn*, Stephen J. Merrill**, and Anita L. Manogaran*†

*Department of Biological Sciences, Marquette University, Milwaukee, WI 53201

**Department of Mathematical and Statistical Sciences, Marquette University, Milwaukee, WI 53201

†Corresponding author: anita.manogaran@marquette.edu, (414) 288-4580, ORCID: 0000-0003-0844-1479

Supplementary Experimental Procedures

Determining the number of cells per colony and stability of known [PIN$^+$] variants

[*pin*$^-$] and high [*PIN*$^+$] 74D-694 strains were subcloned on rich media and grown for 2-3 days at 30^{o}C. 15 colonies were individually picked and resuspended in 1 milliliter of water. The number of cells in a colony was determined by resuspending a 2-3 day old colony in 1 ml of water and determining cell density using a hemocytometer. The number of cells within five square units were counted and number of cells per colony was calculated by the formula = (# of cells in 5 squares X 5) X (10^4). Based on this number, a colony represents on average 20 cell divisions (or generations). Four previously characterized [*PIN*$^+$] variants in the 74D-694 genetic background (low, medium, high, and very high; Bradley et al., 2002) have been shown to be stable, but it was unclear whether their propagation was stable over hundreds of cell divisions. To test propagation stability, we continuously subcloned these four [*PIN*$^+$] variants and tested for maintenance of the prion. In parallel experiments, we also subcloned 74D-694 isogenic [*pin*$^-$], *rnq1Δ,* and *hsp104Δ* strains, all of which do not maintain the prion. After 25 passes of each strain on rich media, consistent with a minimum of 500 cell divisions, strains were transformed with a plasmid containing *RNQ1-GFP*, and cultures were scored for the presence of Rnq1-GFP aggregates.

Determining the axis length of actin mutants

Cell length was obtained through bright field microscopy images of the indicated wildtype and actin mutant BY4741 strains grown in liquid culture for 16 hours. The longest axis length was measured using Leica LASX software. Cultures were blinded,

imaged, and measured in triplicate (n>130). Cell sizes of mutants were significantly larger than wildtype as determined by an unpaired two-tailed t-test ($p<0.0001$).

Rhodamine-Phalloidin staining

Actin polarization during S/G2 phase of the cell cycle was assayed in wildtype and actin mutant strains using rhodamine-phalloidin staining. Briefly, cells were grown to log phase in YPD liquid at 30°C, and then treated with 4% formaldehyde at room temperature for 10 minutes. Samples were washed twice in PBS, and then treated with 6.6μM rhodamine-phalloidin for 1 hour. Samples were washed three times and re-suspended in 100μL of PBS for imaging. To determine actin patch polarization, image files were analyzed blind by an independent investigator, first identifying all S/G2-phase cells in a given (DIC) field, and then examining the rhodamine fluorescence channel through the z-stacks to score for polarization. Cells were classified as polarized (<75% of the actin patches in the daughter bud), partial polarized (50-75% of actin patches in daughter bud), or unpolarized (equal distribution of actin patches in mother cell and daughter bud). Cells with weak to no staining were eliminated from analysis.

de novo [*PSI*$^+$] *formation*

de novo [*PSI*$^+$] induction was performed by transforming strains with a plasmid that contains the prion domain of Sup35 fused to GFP and under a *pCUP1* promoter (*CEN, HIS3, pCUP-SUP35PrD-GFP,* p3031). For C10B-H49 strains, strains were grown for 24 hours in liquid SD-HIS media supplemented with 25 μM copper sulfate. BY4741 strains were grown for 48 hours in liquid SD-HIS media supplemented with 50

μM copper sulfate. Both strains were plated on media that allows for the scoring of [*PSI*$^+$] (see below) and allowed to grow for several days at 30^{o}C.

Two genetic mutations exist within the C10B-H49 background: the *ade2-1* point mutation and a tRNA suppressor, *SUQ5.* Together, these two mutations allow for the [*PSI*$^+$] suppressible phenotype, in which reduced amount of Sup35 protein is available for translation termination of an *ochre* nonsense mutation found in the mutant *ADE2* gene, leading to translational readthrough (Cox, 1965; Liebman et al., 1975; Ter-Avanesyan et al., 1994). Therefore, [*PSI*$^+$], but not [*psi*$^-$], cells grow on SD–Ade media. In contrast, the BY4741 background lacks a [*PSI*$^+$] suppressible allele. Thus, we transformed strains in the BY4741 background with a plasmid carrying the *ura3-14* [*PSI*$^+$] suppressible mutation (*CEN, LEU2, ura3-14; p3107)*, which allows for the detection of [*PSI*$^+$] cells by growth on SD–Leu-Ura media (Manogaran et al., 2006). Comparisons between C10B-H49 strains were performed using an unpaired two-tailed t-test. Results were considered statistically significant with a p-value less than 0.01.

Supplementary Figures

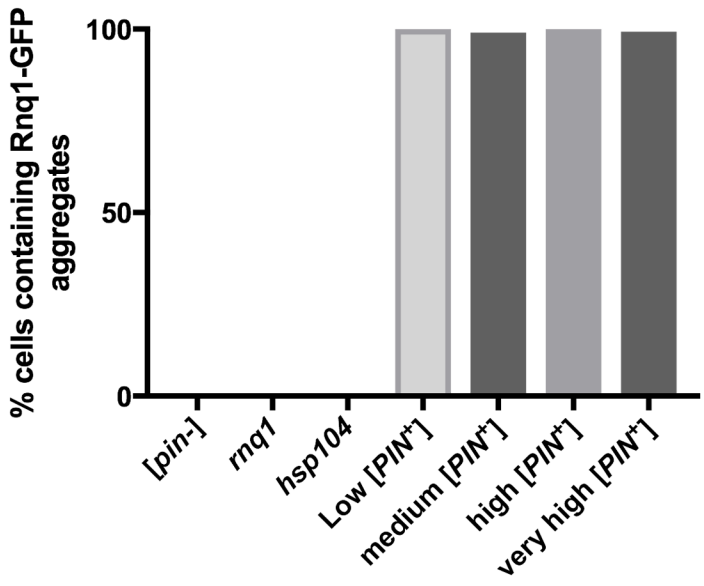

Supplemental Figure 1. Known variants of [*PIN*$^+$] are stable, even after 500 generations. The indicated strains in the 74D-694 genetic background were passed on rich media for 500 generations. *RNQ1-GFP* (p3034) was transformed into each strain and transiently overexpressed to score for the presence of cells containing fluorescent aggregates, as an indicator of [*PIN*$^+$] status. Each bar represents over 300 cells from a single colony.

Supplemental Figure 2. Rnq1-GFP aggregates in Wild type C10B-H49 (represented by cell *a* in Figure 1) with high [*PIN*$^+$]. See supplemental video. Cells transformed with the *pCUP-RNQ1-GFP* plasmid *(p3034)* were grown in SD-His media supplemented with 25 μM Copper Sulfate for 4-6 hours. Cells were imaged in one plane over 10 seconds at 1000X magnification.

Supplemental Figure 3. Rnq1-GFP aggregates in Wild type BY4741 (represented by cell *b* in Figure 1) cytoduced with high [*PIN*$^+$]. See supplemental video. Cells imaged similar to Fig. S2.

Supplemental Figure 4. Rnq1-GFP aggregates in Wild type C10B-H49 cytoduced with high [*PIN*$^+$] from BY4741 donors (represented by cell *c* in Figure 1). See supplemental video. Cells imaged similar to Fig. S2.

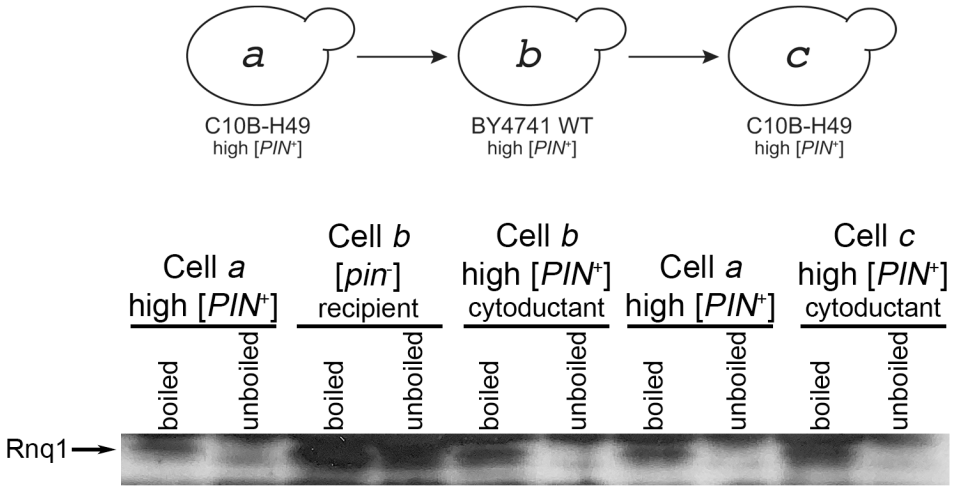

Supplemental Figure 5. SDS-PAGE demonstrates presence of monomeric Rnq1p in [*pin*$^-$] strains. Lysates of the indicated strains were boiled or incubated at room temperature (unboiled) for 10 minutes prior to loading on SDS-PAGE. Under normal conditions, the Rnq1 protein is soluble in [*pin*$^-$] strains, but forms SDS-resistant aggregates in [*PIN*$^+$] strains. Boiling [*PIN*$^+$] lysates in the presence of SDS resolves Rnq1 monomers by Western blot. As expected, unboiled lysates of [*pin*$^-$] strains resolve Rnq1 as a monomer, but [*PIN*$^+$] strains do not. Representative image is shown.

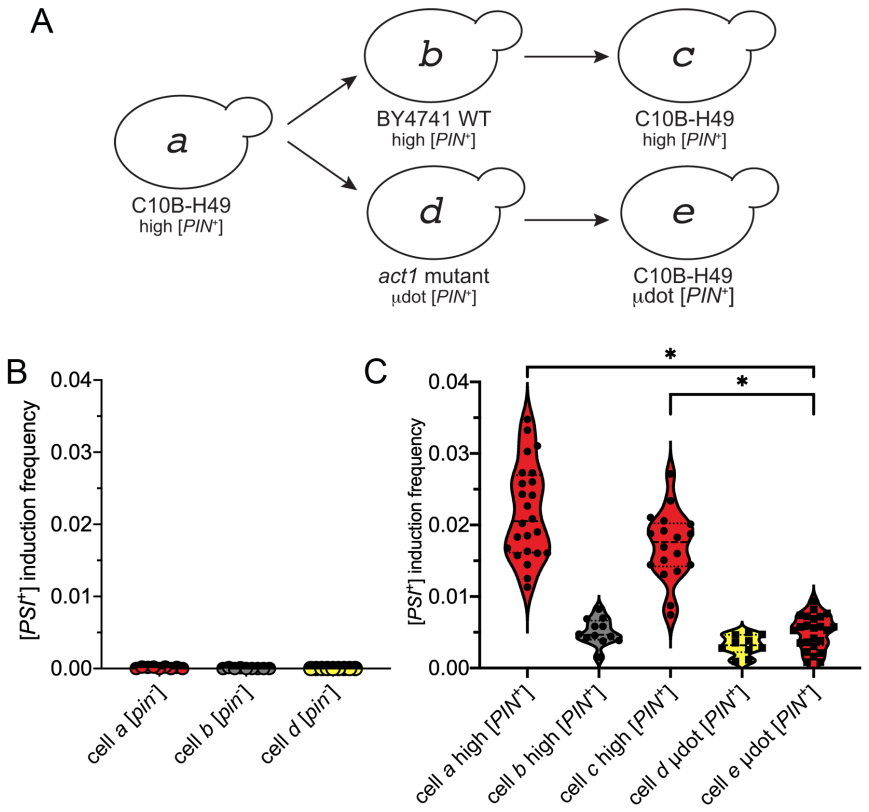

Supplemental Figure 6. Induction of the [*PSI*$^+$] prion occurs in strains with μdot [*PIN*$^+$]. A. Cytoduction scheme of high [*PIN*$^+$] and μdot [*PIN*$^+$]. B. [*PSI*$^+$] induction was tested in [*pin*$^-$] strains by transiently overexpressing Sup35PrD-GFP and plating on [*PSI*$^+$] selective media. [*PSI*$^+$] scoring in the C10B-H49 genetic background (represented by cell *a* [*pin*$^-$], red) relied upon the endogenous [*PSI*$^+$] suppressible *ade2-1* allele, and scoring in the BY4741 background (wild type BY4741 cell *b* [*pin*$^-$] in grey; and *act1-122* BY4741 cell *d* [*pin*$^-$] in yellow) relied upon a plasmid containing a [*PSI*$^+$] suppressible *ura3-14* allele (Manogaran et al., 2010). [*PSI*$^+$] induction was virtually undetectable in all three [*pin*$^-$] strains, consistent with observations by (Lancaster et al., 2010). C. [*PSI*$^+$] induction was tested in the indicated [*PIN*$^+$] strains by transiently overexpressing Sup35PrD-GFP and plating on [*PSI*$^+$] selective media. [*PSI*$^+$] scoring in the C10B-H49 genetic background (represented by cells *a, c* and *e*, respectively) relied upon the endogenous [*PSI*$^+$] suppressible *ade2-1* and *SUQ5* allele, and scoring in the BY4741 background (wildtype BY4741 cell *b* in grey and *act1-122* BY4741 cell *d* in yellow, respectively) relied upon a plasmid containing a [*PSI*$^+$] suppressible *pLEU2ura3-14* allele (Manogaran et al., 2006). Cells *d* and *e* are labeled as μdot [*PIN*$^+$] based upon presence of the μ.d. aggregation phenotype, and further supported as representing a unique variant relative to high [*PIN*$^+$] based upon differential [*PSI*$^+$] inducing abilities within the C10B-H49 genetic background (cells *c* versus *e*, red). Violin plots show all points. Comparisons were performed between C10B-H49 strains only, * $p<0.001$.

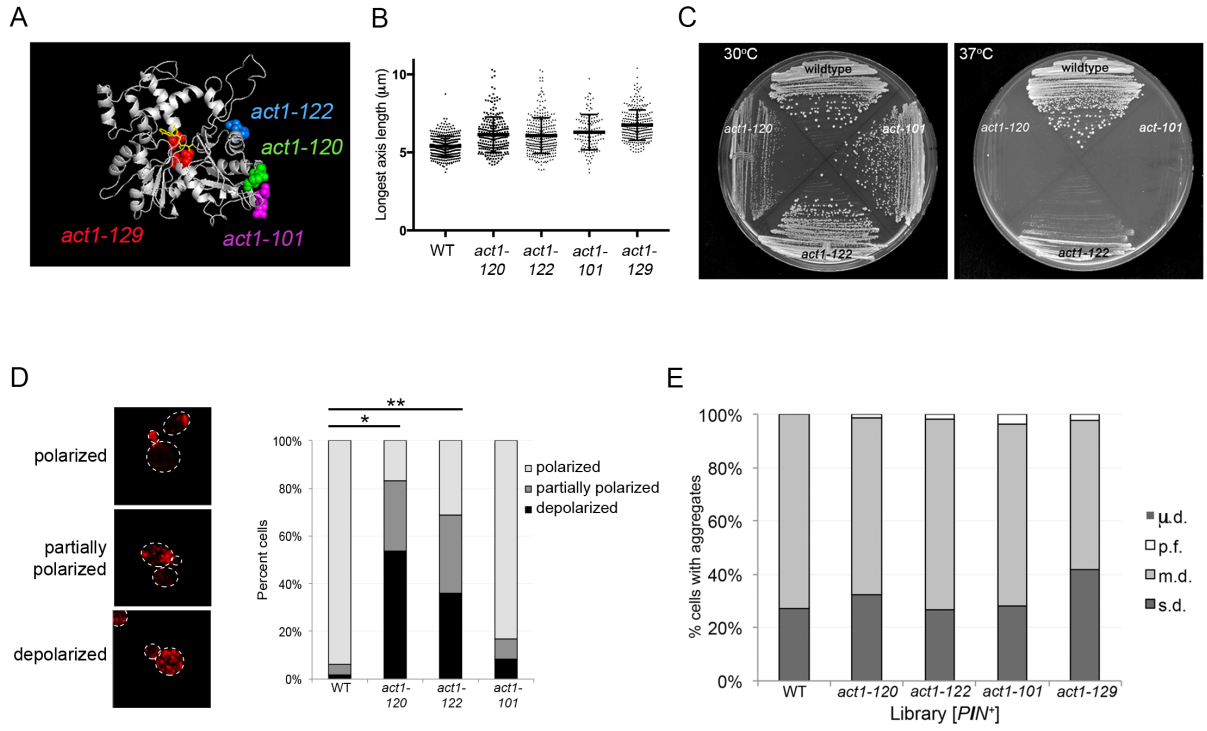

Supplemental Figure 7. Actin mutants in BY4741 show subtle phenotypes at permissive temperatures. A. The structure of the actin protein (PDB ID:3J8I) with highlighted amino acids corresponding to those residues mutated in the *act1-120* (E99A, E100A; green), *act1-122* (D80A, D81A; blue), *act1-129* (R177A, D179A; red), and *act1-101* (D363A, E364A; purple) strains. The bound ADP nucleotide is shown in yellow. B. Strains, in triplicate, were inoculated into liquid medium, grown to late log phase to determine cell size. The mother cell in at least 125 S/G2 phase cells was measured on the long axis of the cell in µm. The size distribution of axis length is shown. C. WT, *act1-120*, *act1-122*, and *act1-101* strains were grown at 30°C (left) and 37°C (right) on rich media for two days. D. Actin polarization was assessed by staining cells with rhodamine-phalloidin. In G2/M phase cells, normal actin patch polarization to the daughter bud (top), partial actin patch polarization (middle), and unpolarized actin patches (bottom) are shown. Approximately 100 G2/M phase cells from each mutant were analyzed in triplicate cultures grown at permissive temperature. Chi-square analysis shows that polarization of *act1-120* and *act1-122* cells were significantly different than wildtype ($p<0.0001$). E. Indicated BY4741 strains containing the library [*PIN*$^+$] variant, which was previously described found in the BY4741 deletion library (Manogaran et al., 2010), were transformed with *RNQ1-GFP* plasmid (p3034) and assayed Rnq1-GFP aggregate type (as described for Figures 1B, 2A, and 3C). Aggregate profiles are comparable among all five strains.

Supplemental Figure 8. Rnq1-GFP aggregates in BY4741 *act1-122* containing μdot [*PIN*$^+$] (represented by cell *d*). See supplemental video. Cells imaged similar to Fig. S2.

Supplemental Figure 9. Rnq1-GFP aggregates in C10B-H49 containing μdot [*PIN*$^+$] (represented by cell *e*). See supplemental video. Cells imaged similar to Fig. S2.

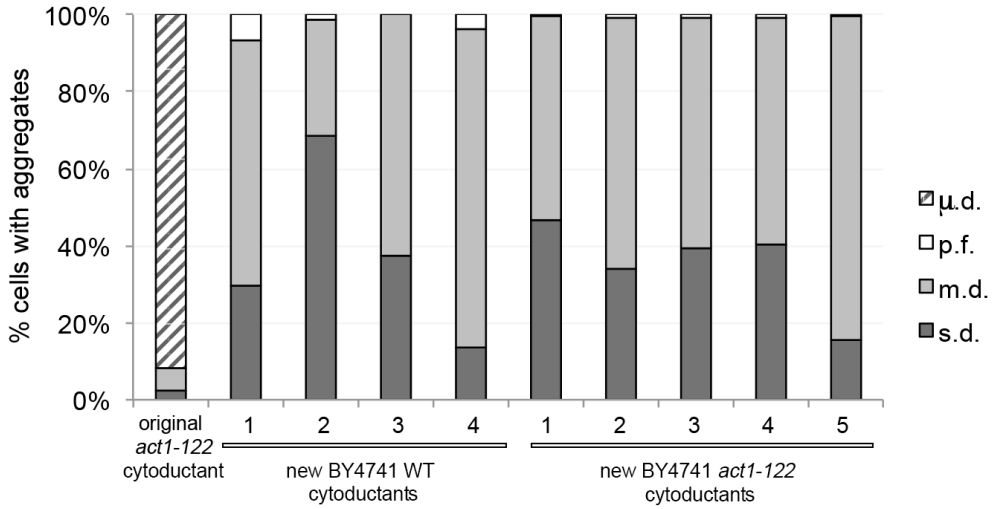

Supplemental Figure 10. Repeated cytoduction of high [*PIN*$^+$] from C10B-H49 (cell *a*) into BY4741 wildtype (cell *b*) or *act1-122* (cell *d*) backgrounds does not generate μ.d. aggregation phenotype. High [*PIN*$^+$] from C10B-H49 (cell *a*) strains were cytoduced again into either BY4741 wildtype or *act1-122* mutant strains. Rnq1-GFP aggregate phenotypes were assessed (as described for Figures 1B, 2A, and 3C). A minimum of 300 cells were assessed for each cytoductant.

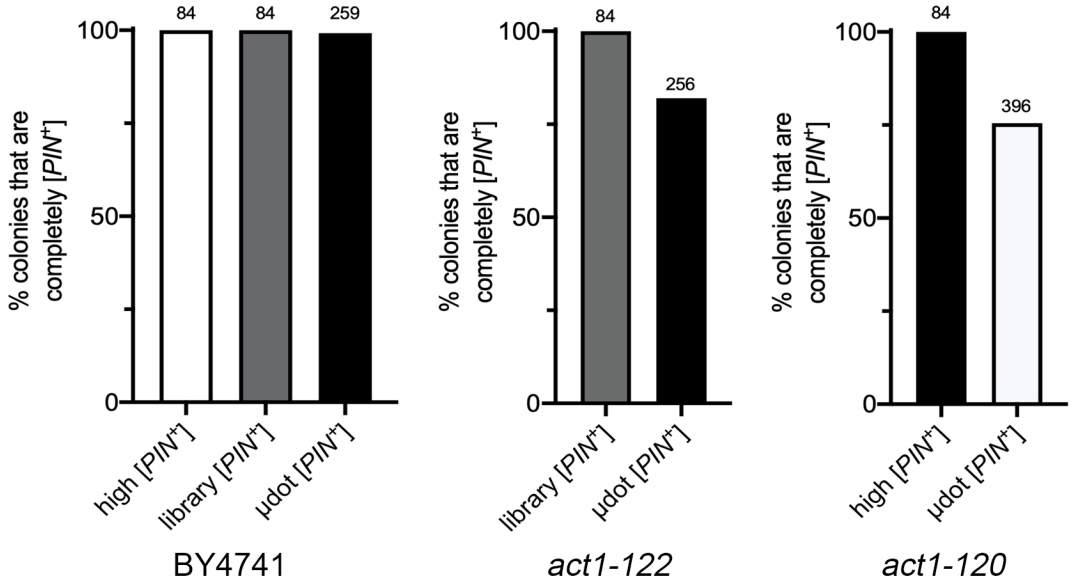

Supplemental figure 11. High and library [*PIN*$^+$] are maintained in *act1-122* and *act1-120* mutants. The indicated BY4741, *act1-122*, or *act1-120* strains containing the specified [*PIN*$^+$] variants were propagated for approximately 100 generations. Individual colonies were assayed for prion loss by mating with a Rnq1-GFP tester strain and scored for presence of Rnq1-GFP aggregates in the cell population, similar to Figure 5.

Supplementary Tables:

Supplemental Table 1. Strains used in this study

Strain name	Genotype	Lab strain number(s)	Plasmid	Reference
Wild type C10B-H49 high [*PIN*$^+$] Cytoduction Donor (cell *a*)	*MAT*α *SUQ5; ade2-1; lys1-1; his3-11,15; leu1; kar1-1; cyhR* high [*PIN*$^+$]	D127		(Bradley and Liebman, 2003)
Wild type BY4741 high [*PIN*$^+$] (cell *b*, with plasmid)	*MatA his3Δ1; leu2Δ-0; ura3Δ-0; met15Δ-0* high [*PIN*$^+$] + p3034 (*RNQ1-GFP; HIS3*)	M232	p3034	This study (Fig. 1,5)
Wild type BY4741 high [*PIN*$^+$] (cell *b*, no plasmid)	*MatA his3Δ1; leu2Δ-0; ura3Δ-0; met15Δ-0* high [*PIN*$^+$]	M361-M362		This study (Fig. 1,5)
Wild type C10B-H49 [*pin*-] recipient (for cells *c* and *e*)	*MAT*α *SUQ5; ade2-1; lys1-1; his3-11,15; leu1; kar1-1; cyhR* [*pin*$^-$], [*psi*$^-$], [*rho*^{0}]	D101		(Kochneva-Pervukhova et al., 1998), (Fig 1C)
Wild type C10B-H49 cytoductant high [*PIN*$^+$] (cell *c*)	*MAT*α *SUQ5; ade2-1; lys1-1; his3-11,15; leu1; kar1-1; cyhR,* high [*PIN*$^+$]	M366, M367, M480, M481		This study (Fig. 1,5)
act1-122 BY4741 μdot [*PIN*$^+$] (cell *d*, with plasmid)	*MatA his3Δ1; leu2Δ-0; ura3Δ-0; act1-122::NATr; MET15; LYS2;* μdot [*PIN*$^+$] + p3034 (*RNQ1-GFP; HIS3*)	M231	p3034	This study (Fig. 2-5)
act1-122 BY4741 μdot [*PIN*$^+$] (cell *d*; no plasmid)	*MatA his3Δ1; leu2Δ-0; ura3Δ-0; act1-122::NATr; MET15; LYS2;* μdot [*PIN*$^+$]	M363-M365		This study (Fig. 3;5,6)
act1-101 BY4741 high [*PIN*$^+$] (with plasmid)	*MatA his3Δ1; leu2Δ-0; ura3Δ-0; act1-101::NATr; met15Δ; LYS2;* high [*PIN*$^+$] + p3034 (*RNQ1-GFP; HIS3*)	M233	p3034	This study (Fig. 2)
act1-120 BY4741 high [*PIN*$^+$] (with plasmid)	*MatA his3Δ1; leu2Δ-0; ura3Δ-0; act1-120::NATr; MET15; LYS2;* high [*PIN*$^+$] + p3034 (*RNQ1-GFP; HIS3*)	M234	p3034	This study (Fig. 2)
act1-129 BY4741 high [*PIN*$^+$] (with plasmid)	*MatA his3Δ1; leu2Δ-0; ura3Δ-0; act1-129::NATr; met15Δ; LYS2;* high [*PIN*$^+$] + p3034 (*RNQ1-GFP; HIS3*)	M235	p3034	This study (Fig. 2)
Tester Strain	*MAT*α *trp1 leu2 ura2*	D163		(Edskes et al., 1999)
Wild type C10B-H49 μdot. [*PIN*$^+$] (cell *e*, no plasmid)	*MAT*α *SUQ5; ade2-1; lys1-1; his3-11,15; leu1; kar1-1; cyhR* μdot. [*PIN*$^+$]	M368, M369, M476-M479		This study (Fig. 3 – 6)
Wild type C10B-H49 μdot. [*PIN*$^+$] (cell *e*) with plasmid	*MAT*α *SUQ5; ade2-1; lys1-1; his3-11,15; leu1; kar1-1; cyhR* μdot. [*PIN*$^+$] + p3034 (*RNQ1-GFP; HIS3*)	M581, M582	p3034	This study (Fig. 3 – 4)
Wild type BY4741 μdot [*PIN*$^+$] (cell *f*, with plasmid)	*MatA his3Δ1; leu2Δ-0; ura3Δ-0; met15Δ-0* μdot [*PIN*$^+$] + p3034 (*RNQ1-GFP; HIS3*)	M394-M396	p3034	This study (Fig. 5)

Wild type BY4741 μdot [*PIN*$^+$] (cell *f*, no plasmid)	*MatA his3Δ1; leu2Δ-0; ura3Δ-0; met15Δ-0* μdot [*PIN*$^+$]	M403-M405		This study (Fig. 5)
act1-122 BY4741 μdot [*PIN*$^+$] (cell *g*, with plasmid)	*MatA his3Δ1; leu2Δ-0; ura3Δ-0; act1-122::NATr; MET15; LYS2* μdot [*PIN*$^+$] + p3034 (*RNQ1-GFP; HIS3*)	M397, M398	p3034	This study (Fig. 5)
act1-122 BY4741 μdot [*PIN*$^+$] (cell *g*, no plasmid)	*MatA his3Δ1; leu2Δ-0; ura3Δ-0; act1-122::NATr; MET15; LYS2* μdot [*PIN*$^+$]	M399-M402		This study (Fig. 5 & 6)
act1-122 BY4741 μdot [*PIN*$^+$] (cell *g*; no plasmid; 60 generations)	*MatA his3Δ1; leu2Δ-0; ura3Δ-0; act1-122::NATr; MET15; LYS2* μdot [*PIN*$^+$]	M452		This study (Fig. 6)
act1-120 BY4741 μdot [*PIN*$^+$] (cell *h*, with plasmid)	*MatA his3Δ1; leu2Δ-0; ura3Δ-0; act1-120::NATr; MET15; LYS2;* μdot [*PIN*$^+$] + p3034 (*RNQ1-GFP; HIS3*)	M579. M580	p3034	This study (Fig. 5)
act1-120 BY4741 μdot [*PIN*$^+$] (cell *h*, no plasmid)	*MatA his3Δ1; leu2Δ-0; ura3Δ-0; act1-120::NATr; MET15; LYS2;* μdot [*PIN*$^+$]	M482–M490		This study (Fig. 5, Trials)

Strains used in supplemental figures:

Wild type 74D-694 high [*PIN*+]	*MatA ade1-14 ura3-52 leu2-3,112 trp1-289 his3-200* high [*PIN*$^+$]	D233		(Derkatch et al., 1997) (S1 Fig)
Wild type 74D-694 low [*PIN*+]	*MatA ade1-14 ura3-52 leu2-3,112 trp1-289 his3-200* low [*PIN*$^+$]	D231		(Bradley et al., 2002) (S1 Fig)
Wild type 74D-694 medium [*PIN*+]	*MatA ade1-14 ura3-52 leu2-3,112 trp1-289 his3-200* medium [*PIN*$^+$]	D232		(Bradley et al., 2002) (S1 Fig)
Wild type 74D-694 very high [*PIN*+]	*MatA ade1-14 ura3-52 leu2-3,112 trp1-289 his3-200* very high [*PIN*$^+$]	D234		(Bradley et al., 2002) (S1 Fig)
Wild type 74D-694 [*pin*$^-$]	*MatA ade1-14 ura3-52 leu2-3,112 trp1-289 his3-200*	D230		(Derkatch et al., 1997) (S1 Fig, and Fig 1D)
rnq1 deletion	*MatA ade1-14 leu2-3,112 ura3-52 trp1-289 his3-200 rnq1::HIS3,* [*pin*$^-$]	M168		(Manogaran et al., 2011) (S1 Fig)
hsp104 deletion	*MatA ade1-14 ura3-52 leu2-3,112 trp1-289 his3-200 hsp104::LEU2 [psi-][pin-]*	D223		(Zhou et al., 2001) (S1 Fig)
BY4741 *act1-120* high [*PIN*$^+$]	*MatA his3Δ1; leu2Δ-0; ura3Δ-0; act1-120::NATr; MET15; LYS2* high [*PIN*$^+$]	M312		This study (S7 Fig)
BY4741 *act1-129* [*PIN*$^+$]	*MatA his3Δ1; leu2Δ-0; ura3Δ-0; act1-129::NATr; met15Δ; LYS2* high [*PIN*$^+$]	M258		This study (S7 Fig)

BY4741 *act1-101* [*PIN*$^+$]	*MatA his3Δ1; leu2Δ-0; ura3Δ-0; act1-101::NATr; met15Δ; LYS2* high [*PIN*$^+$]	M256		This study (S7 Fig)
BY4741 *act1-122* μ.d. [*PIN*$^+$]	*MatA his3Δ1; leu2Δ-0; ura3Δ-0; act1-122::NATr; MET15; LYS2* high [*PIN*$^+$]	M254, M257		This study (S7 Fig)
Wild type BY4741 library [*PIN*$^+$]	*MatA his3Δ1; leu2Δ-0; ura3Δ-0; met15Δ-0* library [*PIN*$^+$]	D181		(Winzeler et al., 1999) (S7E Fig)
BY4741 *act1-101* library [*PIN*$^+$]	*MatA his3Δ1; leu2Δ-0; ura3Δ-0; act1-101::NATr; met15Δ; LYS2* library [*PIN*$^+$]	D190		(Viggiano et al., 2010) (S7E Fig)
BY4741 *act1-120* library [*PIN*$^+$]	*MatA his3Δ1; leu2Δ-0; ura3Δ-0; act1-120::NATr; MET15; LYS2;* library [*PIN*$^+$]	D191		(Viggiano et al., 2010) (S7E Fig)
BY4741 *act1-122* library [*PIN*$^+$]	*MatA his3Δ1; leu2Δ-0; ura3Δ-0; act1-122::NATr; MET15; LYS2* library [*PIN*$^+$]	D192		(Viggiano et al., 2010) (S7E Fig)
BY4741 *act1-129* library [*PIN*$^+$]	*MatA his3Δ1; leu2Δ-0; ura3Δ-0; act1-129::NATr; met15Δ-0; LYS2* library [*PIN*$^+$]	D193		(Viggiano et al., 2010) (S7E Fig)
Wild type BY4741 high [*PIN*$^+$] (result of replicate cytoductions, with plasmid)	*MatA his3Δ1; leu2Δ-0; ura3Δ-0; met15Δ-0* high [*PIN*$^+$] + p3034 (*RNQ1-GFP; HIS3*)	M467-M470	p3034	This study (S10 Fig)
BY4741 *act1-122* high [*PIN*$^+$] (result of replicate cytoductions, with plasmid)	*MatA his3Δ1; leu2Δ-0; ura3Δ-0; act1-122::NATr; MET15; LYS2* high [*PIN*$^+$] + p3034 (*RNQ1-GFP; HIS3*)	M471-M475	p3034	This study (S10 Fig)
act1-120 BY4741 high [*PIN*$^+$]	*MatA his3Δ1; leu2Δ-0; ura3Δ-0; act1-120::NATr; MET15; LYS2;* high [*PIN*$^+$]	M466		This study (S11 Fig)

Supplementary Table 2. Plasmids used in this study

Plasmid name	Lab number	Markers	Reference
pCUP-RNQ1-GFP	*p3034*	*HIS3, CEN*	(Sondheimer and Lindquist, 2000)
pCUP-RNQ1-GFP	*p3036*	*LEU2, CEN*	(Sondheimer and Lindquist, 2000)
pCUP-SUP35PrD-GFP	*p3031*	*HIS3, CEN*	(Zhou et al., 2001)
pLEU2ura3-14	*p3107*	*LEU2, CEN*	(Manogaran et al., 2006)

Reference:

Bradley, M.E., Edskes, H.K., Hong, J.Y., Wickner, R.B., and Liebman, S.W. (2002). Interactions among prions and prion "strains" in yeast. Proc Natl Acad Sci U S A *99 Suppl 4*, 16392-16399.

Bradley, M.E., and Liebman, S.W. (2003). Destabilizing interactions among [PSI(+)] and [PIN(+)] yeast prion variants. Genetics *165*, 1675-1685.

Cox, B.S. (1965). [*PSI*], a cytoplasmic suppressor of super-suppressors in yeast. Heridity *20*.

Derkatch, I.L., Bradley, M.E., Zhou, P., Chernoff, Y.O., and Liebman, S.W. (1997). Genetic and environmental factors affecting the de novo appearance of the [PSI+] prion in Saccharomyces cerevisiae. Genetics *147*, 507-519.

Edskes, H.K., Gray, V.T., and Wickner, R.B. (1999). The [URE3] prion is an aggregated form of Ure2p that can be cured by overexpression of Ure2p fragments. Proc Natl Acad Sci U S A *96*, 1498-1503.

Kochneva-Pervukhova, N.V., Poznyakovski, A.I., Smirnov, V.N., and Ter-Avanesyan, M.D. (1998). C-terminal truncation of the Sup35 protein increases the frequency of de novo generation of a prion-based [PSI+] determinant in Saccharomyces cerevisiae. Curr Genet *34*, 146-151.

Lancaster, A.K., Bardill, J.P., True, H.L., and Masel, J. (2010). The spontaneous appearance rate of the yeast prion [PSI+] and its implications for the evolution of the evolvability properties of the [PSI+] system. Genetics *184*, 393-400.

Liebman, S.W., Stewart, J.W., and Sherman, F. (1975). Serine substitutions caused by an ochre suppressor in yeast. J Mol Biol *94*, 595-610.

Manogaran, A.L., Fajardo, V.M., Reid, R.J., Rothstein, R., and Liebman, S.W. (2010). Most, but not all, yeast strains in the deletion library contain the [PIN(+)] prion. Yeast *27*, 159-166.

Manogaran, A.L., Hong, J.Y., Hufana, J., Tyedmers, J., Lindquist, S., and Liebman, S.W. (2011). Prion formation and polyglutamine aggregation are controlled by two classes of genes. PLoS genetics *7*, e1001386.

Manogaran, A.L., Kirkland, K.T., and Liebman, S.W. (2006). An engineered nonsense URA3 allele provides a versatile system to detect the presence, absence and appearance of the [PSI+] prion in Saccharomyces cerevisiae. Yeast *23*, 141-147.

Sondheimer, N., and Lindquist, S. (2000). Rnq1: an epigenetic modifier of protein function in yeast. Mol Cell *5*, 163-172.

Ter-Avanesyan, M.D., Dagkesamanskaya, A.R., Kushnirov, V.V., and Smirnov, V.N. (1994). The SUP35 omnipotent suppressor gene is involved in the maintenance of the non-Mendelian determinant [psi+] in the yeast Saccharomyces cerevisiae. Genetics *137*, 671-676.

Viggiano, S., Haarer, B., and Amberg, D.C. (2010). Correction/completion of the yeast actin, alanine scan alleles. Genetics *185*, 391-394.

Winzeler, E.A., Shoemaker, D.D., Astromoff, A., Liang, H., Anderson, K., Andre, B., Bangham, R., Benito, R., Boeke, J.D., Bussey, H.*, et al.* (1999). Functional characterization of the S. cerevisiae genome by gene deletion and parallel analysis. Science *285*, 901-906.

Zhou, P., Derkatch, I.L., and Liebman, S.W. (2001). The relationship between visible intracellular aggregates that appear after overexpression of Sup35 and the yeast prion-like elements [PSI(+)] and [PIN(+)]. Mol Microbiol *39*, 37-46.